Nonlinear Modeling Benchmarks of Forced Magnetic Reconnection with NIMROD and M3D-C1

M. T. Beidler[1], J. D. Callen[1], C. C. Hegna[1], C. R. Sovinec[1], N. M. Ferraro[2]

[1]*Department of Engineering Physics, University of Wisconsin*
[2]*Princeton Plasma Physics Laboratory*

Supported by DOE OFES grants DE-FG02-92ER54139, DE-FG02-86ER53218, DE-AC02-09CH11466, the SciDAC Center for Extended MHD Modeling, and the U.S. DOE FES Postdoctoral Research program administered by ORISE and managed by ORAU under DOE contract DE-SC0014664.

Abstract

The nonlinear, extended-magnetohydrodynamic (MHD) code NIMROD is benchmarked with the theory of time-dependent forced magnetic reconnection (FMR) induced by small resonant fields in slab geometry [1] in the context of visco-resistive MHD modeling. Linear computations agree with time-asymptotic, linear theory of flow screening of externally-applied fields [2]. The inclusion of flow in nonlinear computations can result in mode penetration due to the balance between electromagnetic and viscous forces in the time-asymptotic state, which produces bifurcations from a high-slip to a low-slip state as the external field is slowly increased [3]. We reproduce mode penetration and unlocking transitions by employing time-dependent externally-applied magnetic fields. Mode penetration and unlocking exhibit hysteresis and occur at different magnitudes of applied field. We establish how nonlinearly-determined flow screening of resonant field penetration is affected by the externally-applied field amplitude. These results emphasize that inclusion of nonlinear physics is essential for accurate prediction of field penetration in a flowing plasma, as described in a manuscript recently accepted for publication [4]. We explore FMR in cylindrical geometry by way of benchmarks between the NIMROD and M3D-C1 extended-MHD codes. Linear computational results of flow-scaling of field penetration display excellent agreement, and exhibit reasonable agreement with analytical predictions derived for an asymptotic dissipation regime [2]. We also compare nonlinear computations to analytical predictions of quasilinear, time-asymptotic, force balance [3].

[1] T. S. Hahm and R. M. Kulsrud, Phys. Fluids 28, 2412 (1985)
[2] R. Fitzpatrick, Phys. Plasmas 5, 3325 (1998)
[3] R. Fitzpatrick, Nucl. Fusion 33, 1049 (1993)
[4] M. T. Beidler, J. D. Callen, C. C. Hegna, and C. R. Sovinec, “Nonlinear Modeling of Forced Magnetic Reconnection in Slab Geometry with NIMROD,” report UW-CPTC 17-1, 7 March 2017, available via www.cptc.wisc.edu, Accepted to Phys. Plasmas

Motivation

- **External 3D fields force magnetic reconnection (FMR), whose islands can lock plasma in place to 3D field structure**
  - Fundamental physics is controlled by external forcing, flow, resistivity, and viscosity
- **Many simulations of linear flow screening have been performed, but nonlinear torque (force) balance plays role in determining flow**
  - Code verification in slab and cylindrical geometries critical for understanding the general linear and nonlinear responses to applied fields
  - Proceed by applying to realistic physics models and toroidal geometry
- **NIMROD and M3D-C[1] codes evolve extended-MHD models that describe FMR and mode locking physics**
  - Study of FMR with these codes is needed to enhance confidence in computational results

Taylor's Slab Model Paradigm Explored in NIMROD Computations

- **Slab geometry with uniform out-of-plane current density**
  - Stable equilibrium with $\Delta' a \cong -2\pi$
    - $B_{y,0}(x=a) \equiv B_{norm} = 0.1\,T$, $B_{z,0}(x=0) = 100 B_{norm}$
    - $a = L_{norm} = 1\,m$
- **Sinusoidal applied normal magnetic field at edge $B_{x,1}(|x|=a) = B_{ext} \sin(k_y y)$**
  - Drives reconnection at x=0
  - $k_y = 2\pi n / L_y \rightarrow k_y(n=1) = \pi$
- **Visco-Resistive dissipation parameters**
  - $S = 3.5\times10^5$, $P_m = 1$
  - Linear layer width: $\delta_{VR} = S^{-1/3} P_m^{1/6} a = 4.5\times10^{-3} a$
  - Viscosity profile $\sim [1 + (\Delta_{mag}^{1/2} - 1)(x'/a)^{\Delta_{width}}]^2$ with Δ_{mag} =1000 and Δ_{width} =5
- **Gaussian flow profile in x with $v_{y,0}$ at x=0**
  - $v_{norm} = v_A(B_{norm}) = 6.89\times10^5$ m/s $\rightarrow$ $t_{norm} = a / v_{norm} = \tau_A = 1.45\ \mu s$

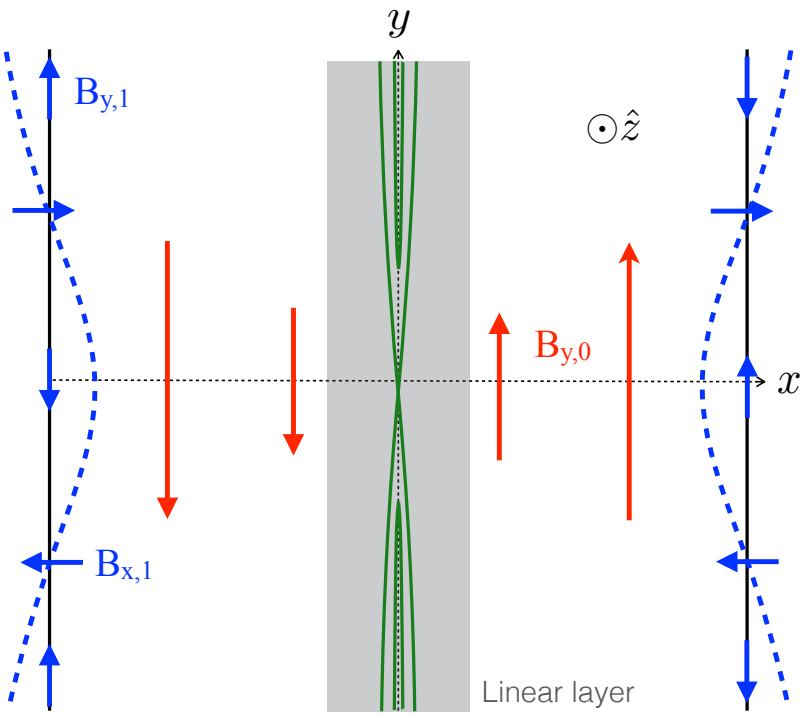

NIMROD Code Employed to Solve Visco-Resistive MHD Equations

- **NIMROD capable of solving extended-MHD equations**
  - Sovinec et al., JCP (2004)
- **Time discretization uses finite difference**
  - Semi-implicit leapfrog time evolution
  - Evolve perturbation fields about a fixed equilibrium

$$\rho\left(\frac{\partial \mathbf{V}}{\partial t}+\mathbf{V}\cdot\boldsymbol{\nabla}\mathbf{V}\right)=\mathbf{J}\times\mathbf{B}-\boldsymbol{\nabla}\cdot\boldsymbol{\Pi}_i,$$

$$\boldsymbol{\Pi}_i\equiv-\rho\nu\left[\boldsymbol{\nabla}\mathbf{V}+\boldsymbol{\nabla}\mathbf{V}^T-\frac{2}{3}\boldsymbol{\nabla}\cdot\mathbf{V}\right],$$

$$\frac{\partial \mathbf{B}}{\partial t}=-\boldsymbol{\nabla}\times\mathbf{E}+\kappa_{divbd}\boldsymbol{\nabla}\boldsymbol{\nabla}\cdot\mathbf{B},$$

$$\mathbf{E}=-\mathbf{V}\times\mathbf{B}+\eta\mathbf{J},$$

$$\mu_0\mathbf{J}=\boldsymbol{\nabla}\times\mathbf{B}$$

- **Spatial discretization uses 2D C^0 finite elements with finite Fourier series in 3rd dimension:**

$$\mathbf{N}(x,y,z,t)=\mathbf{N}_0(x,y,t)+\sum_{n=1}\left[\mathbf{N}_n(x,y,t)e^{i\frac{2\pi n}{L_z}z}+\mathbf{N}_n^*(x,y,t)e^{-i\frac{2\pi n}{L_z}z}\right]$$

- **Numerical divergence error 'cleaner' in Faraday's law**

Computed Linear Plasma Response to Flow Agrees with Fitzpatrick Predictions

- **Blue dots, lines are linear slab analytics adapted from Fitzpatrick, POP (1998)**

$$B_{\mathrm{res}} = \frac{a\Delta'_{\mathrm{ext}}}{-a\Delta' - i\omega_0\tau_\delta} B_{\mathrm{ext}}$$

  - B_{res} is penetrated field at x=0
  - $\Delta'_{\mathrm{ext}} a = 2k_y a/\sinh(k_y a) = 0.544$ is tearing drive due to B_{ext}
  - $\omega_0\tau_A = k_y v_{y,0}\tau_A < 4.56\times10^{-3} \rightarrow Q_0 \equiv \tau_A S^{1/3}\omega_0 < 0.319 < 1$
  - $\tau_\delta \equiv \tau_{VR} = 2.104\tau_A\, S^{2/3} P_m^{1/6}$

    $= 1.03\times10^4\, \tau_A$

- **Red stars, lines are computational results from NIMROD**
  - $B_{ext} = 2\times10^{-5}\, B_{norm}$
  - $\pi/2$ corresponds to B_{res} out-of-phase with B_{ext}

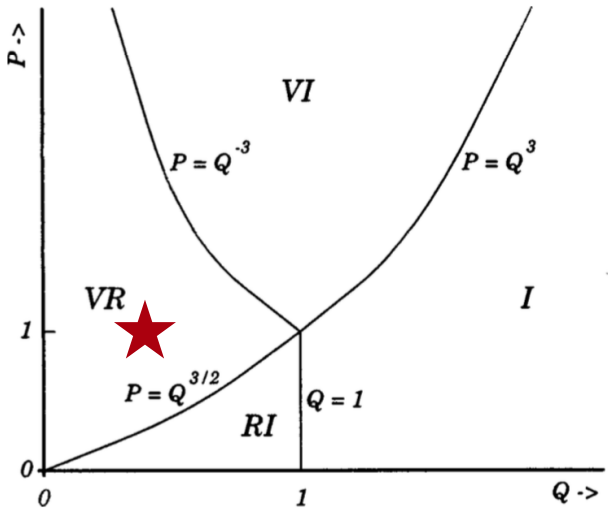

Electromagnetic and Viscous Force Balance Gives Rise to Bifurcation

- **Quasilinear n = 0 electromagnetic and viscous forces per unit length in z at x=0 [e.g. Fitzpatrick, NF (1993)]**

$$\hat{F}_{y,EM} = \frac{\omega_{\rm res}\tau_{\rm VR}}{(a\Delta')^2 + (\omega_{\rm res}\tau_{\rm VR})^2} \frac{\pi n (a\Delta'_{\rm ext})^2}{a k_y^2} \frac{B_{\rm ext}^2}{\mu_0}$$

$$\hat{F}_{y,VS} = -\frac{4\pi n \rho \nu(x=0)}{\nu_{\rm int} a k_y^2}(\omega_0 - \omega_{\rm res})$$

  - **$\omega_{\rm res}$ is flow frequency at x=0**
  - **Viscosity profile-scaling**

$$\nu_{int} = \frac{1}{a}\int_0^a \frac{dx'}{[1 + (\Delta_{\rm mag}^{1/2} - 1)(x'/a)^{\Delta_{\rm width}}]^2} = 0.431$$

  - $\hat{F}_{\rm norm} = \rho v_{\rm norm} a^2 / t_{\rm norm} = 7.94\,{\rm kN/m}$

- **Force balance yields cubic relation in $\omega_{\rm res}$**

$$\frac{\omega_0}{\omega_{\rm res}} - 1 + \omega_0\omega_{\rm res}\tau'^2_{\rm VR} - \omega^2_{\rm res}\tau'^2_{\rm VR} = \frac{\nu_{\rm int}\tau_{\rm VR}}{4\rho\nu(x=0)}\left(\frac{\Delta'_{\rm ext}}{-\Delta'}\right)^2 \frac{B^2_{\rm ext}}{\mu_0}$$

  - $\tau'_{\rm VR} = \tau_{\rm VR}/(-a\Delta')$ **and** $w_{\rm island} \equiv 4\sqrt{\dfrac{aB_{\rm res}}{k_y B_{y,0}(x=a)}}$

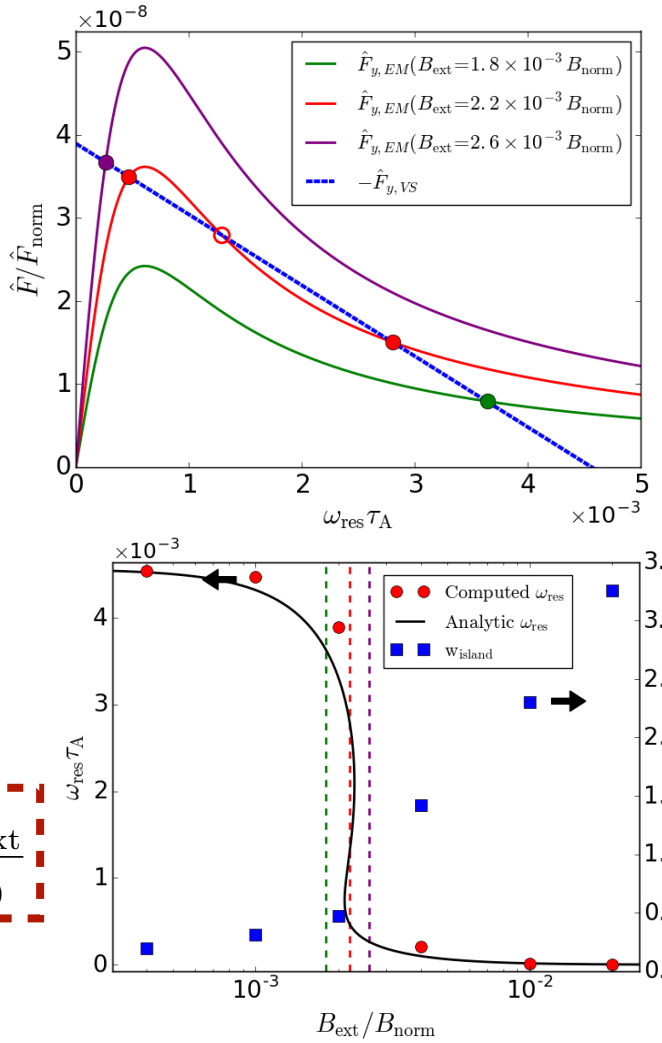

Time-Asymptotic States in Slab Geometry are Consistent with Analytics of Mode Penetration

- **Quasilinear force balance yields transition from high-slip to low-slip state for increasing B_{ext}**
  - a) $B_{ext} = 2\times10^{-3}\, B_{norm}$
  - b) $B_{ext} = 4\times10^{-3}\, B_{norm}$
- **Low-slip state exhibits mode penetration in phase with B_{ext}**
- **$w_{island} > \delta_{VR}$ in low-slip state**
  - Quasilinear EM force should be replaced with modified Rutherford equation

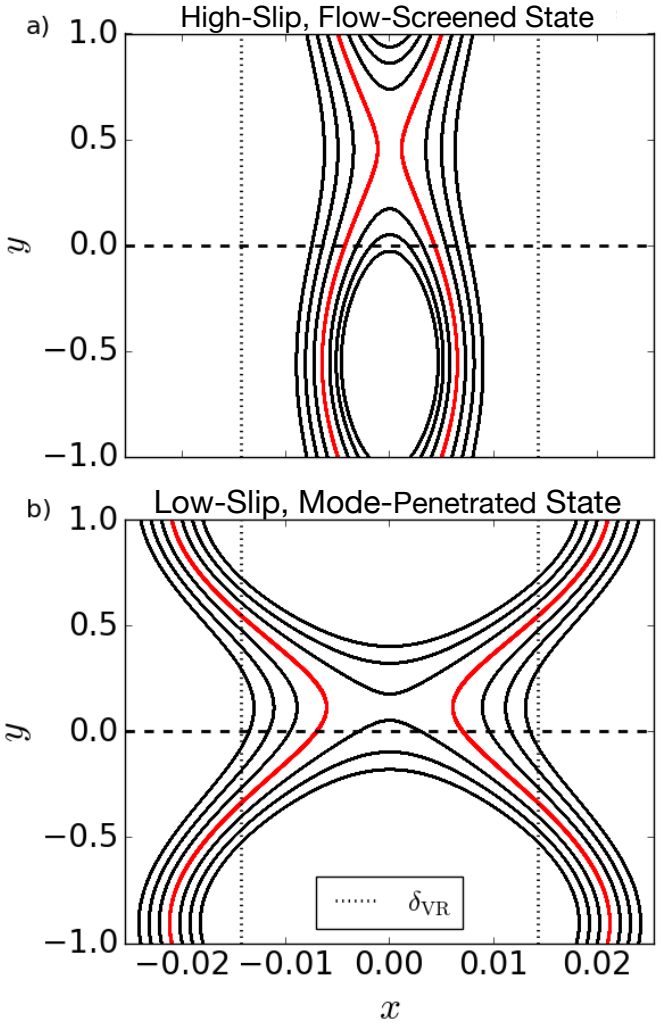

NIMROD Computations Exhibit Hysteresis with Time-Dependent Applied Field

- **System bifurcates and exhibits hysteresis for** $\omega_0 > \omega_{0,\mathrm{crit}} = 3\sqrt{3}/\tau'_{\mathrm{VR}}$
  - Blue curve in top left plot has $\omega_0 \tau'_{\mathrm{VR}} \sim 25$
- **Quasilinear force balance yields $B_{ext,pen\{unlock\}} = 2.89\,\{1.58\} \times 10^{-3}\, B_{norm}$**
  - Middle left plot shows mode penetration
  - Bottom left plot shows mode unlocking
- **Computational results reminiscent of DIII-D experimental observations**
  - Unlocking of n=1 mode as n=2 RMP intensity decreased in two lower plots on right

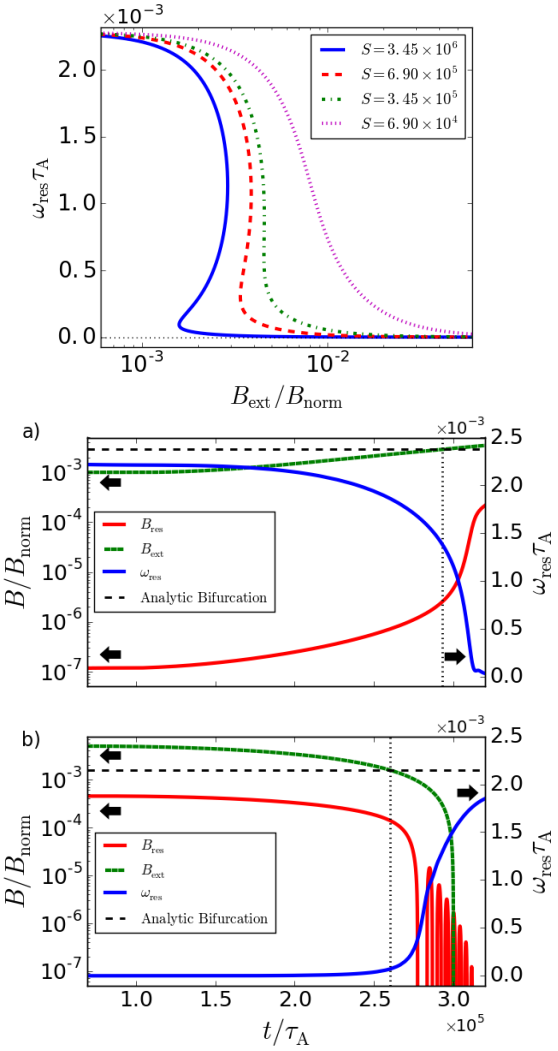

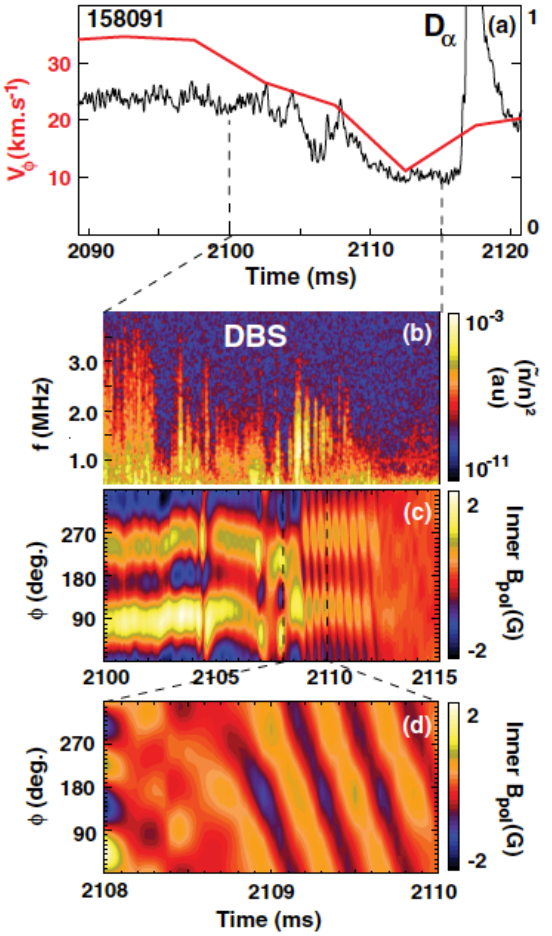

Nazikian, PRL (2015) Fig. 5

Unlocked Magnetic Island Advects Relative to External Field

- **Consistent with prediction in Fitzpatrick, NF (1993)**
  - Advection of unlocked island relative to external field leads to flow screening
- **Island advects with flow frequency $\omega_{unlock}\tau_A$ =1.03×10^{-3}**
  - Flow increases as B_{ext} decreases
- **Additional compression of island occurs when out of phase with external perturbation**

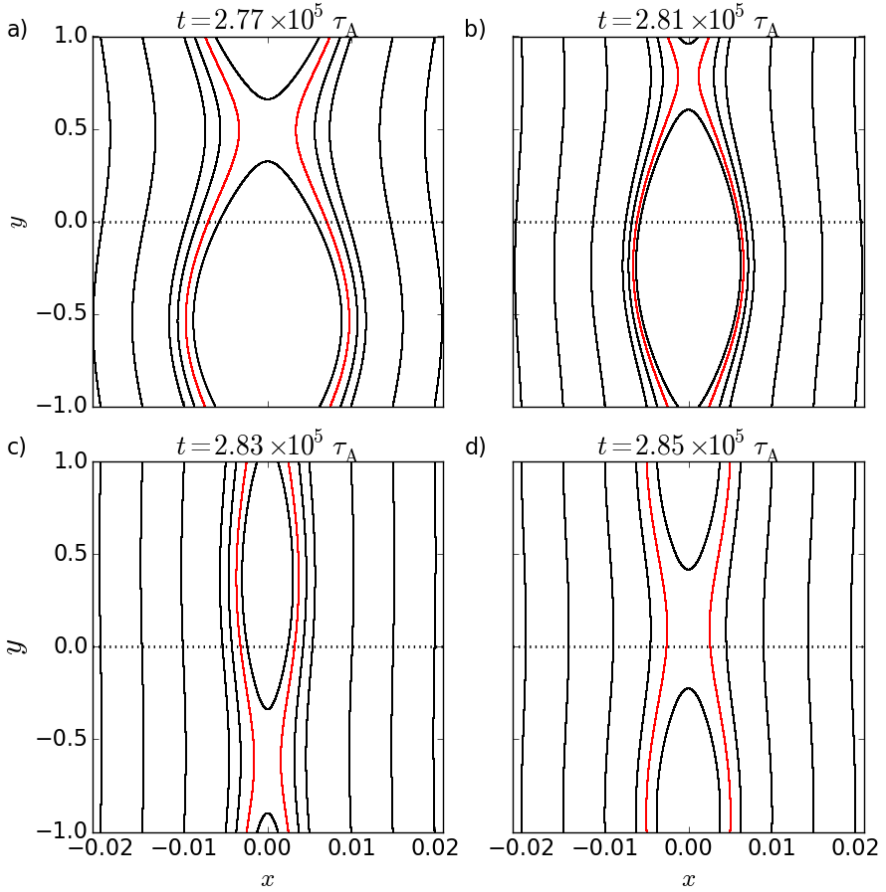

Nonlinear Field Response is Increased from Linear Response

- **As B_{ext} increases, flow at resonant surface decreases**

$$\left(\frac{\omega_0}{\omega_{\rm res}}-1\right)\left(1+\omega_{\rm res}^2\tau_{\rm VR}'^2\right)=\frac{\nu_{\rm int}\tau_{\rm VR}}{4\rho\nu(x=0)}\left(\frac{\Delta_{\rm ext}'}{-\Delta'}\right)^2\frac{B_{\rm ext}^2}{\mu_0}$$
$$\equiv A_{\rm RHS}B_{\rm ext}^2$$

  - ω_{res}/ω_0 decreases from unity

- **Existence of bifurcations (at $\omega_{res} = \omega_0/2$) give rise to discontinuous jump in ω_{res} and B_{res}**

  - When external forcing satisfies

$$B_{\rm ext} > B_{\rm ext,lock}(\omega_{0,\rm crit}) = \frac{1}{2}\sqrt{\frac{4+\omega_{0,\rm crit}^2\tau_{\rm VR}'^2}{A_{\rm RHS}}}$$
$$= 1.65\times10^{-3}\,B_{\rm norm}$$

- **Computations approach nexus of different asymptotic dissipative regimes as ω_0 is increased**

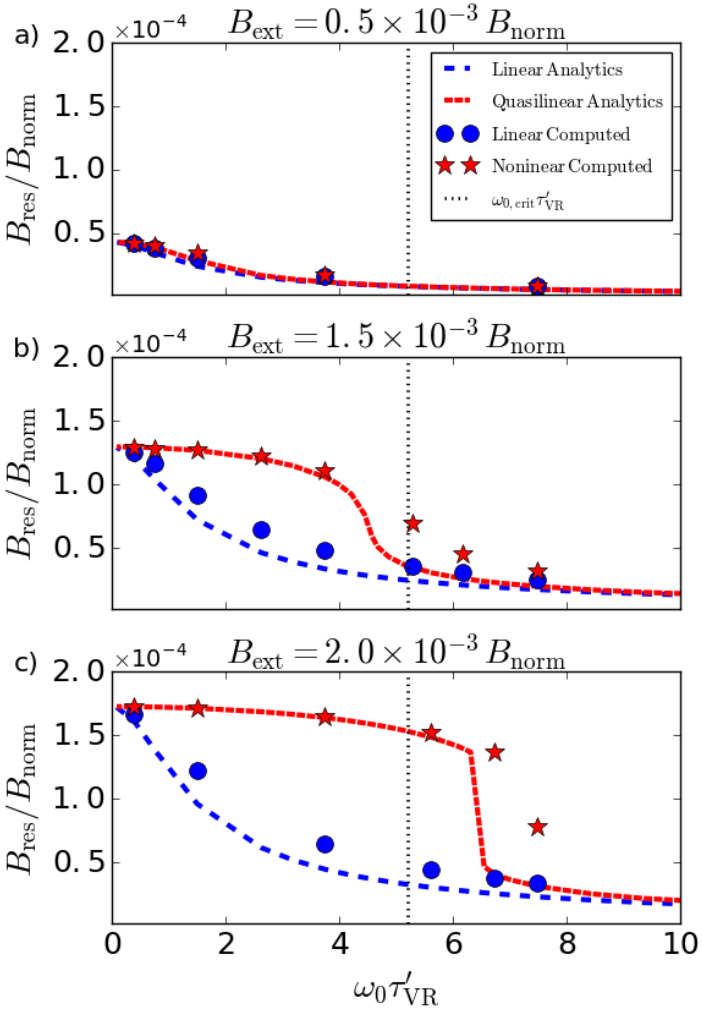

NIMROD and M3D-C1 Solve Visco-Resistive MHD Equations

System of Equations

- $\frac{\partial n}{\partial t} + \nabla \cdot (n\mathbf{V}) = \nabla \cdot D\nabla n,$
- $\rho\left(\frac{\partial \mathbf{V}}{\partial t} + \mathbf{V}\cdot\nabla\mathbf{V}\right) = \mathbf{J}\times\mathbf{B} - \nabla p - \nabla\cdot\Pi_i,$
- $\Pi_i = -\mu\left(\nabla\mathbf{V} + \nabla\mathbf{V}^T - \frac{2}{3}\nabla\cdot\mathbf{V}\right),$
- $\mathbf{E} + \mathbf{V}\times\mathbf{B} = \eta\mathbf{J},$
- $\frac{3}{2}\left[\frac{\partial p}{\partial t} + \nabla\cdot(p\mathbf{V})\right] = -p\nabla\cdot\mathbf{V} + \nabla\cdot n\chi\nabla T,$
- $\frac{\partial \mathbf{B}}{\partial t} = -\nabla\times\mathbf{E} + \kappa_{divbd}\nabla\nabla\cdot\mathbf{B},$ NIMROD only
- $\mu_0\mathbf{J} = \nabla\times\mathbf{B}$

Field Representation

- **NIMROD: 2D spectral, 1D Fourier, vector variables**

$$\mathbf{N}(x,y,z,t) = \mathbf{N}_0(x,y,t) + \sum_{n=1}\left[\mathbf{N}_n(x,y,t)e^{i\frac{2\pi n}{L_z}z} + \mathbf{N}_n^*(x,y,t)e^{-i\frac{2\pi n}{L_z}z}\right]$$

- **M3D-C^1: 3D finite element, scalar variables**

$$\mathbf{A} = R^2\nabla\phi\times\nabla f + \psi\nabla\phi - F_0\ln R\hat{Z}$$

$$\mathbf{B} = \nabla\psi\times\nabla\phi - \nabla_\perp\frac{\partial f}{\partial\phi} + F\nabla\phi$$

$$F = F_0 + R^2\nabla\cdot\nabla_\perp f$$

$$\mathbf{V} = R^2\nabla U\times\nabla\phi + R^2\omega\nabla\phi + \frac{1}{R^2}\nabla_\perp\chi$$

Linear Cylindrical FMR Benchmark is Underway

- **Employ axial current profile** $j_z(r) = j_{z0}\left[1 - \left(\frac{r}{a}\right)^2\right]^{\nu}$
  - RESTER calculates equilibria with $q(r=0) \leq 3$ are resistively unstable ($\Delta' > 0$)
    - Use $q(r=0)=3.08$ to avoid tearing modes
  - $j_{z0} = 0.103$ MA/m^2, $\nu = 1.50$, $B_{z0} = 1\text{T} \equiv B_{norm}$, $R_0 = 5\text{m}$, $q(r=a)=7.68$, $r(q=4) \equiv r_s = 0.572\text{m}$
  - RESTER calculates $r_s\Delta'_{q=4} = -2.52$
- **Helical (m,n)=(4,1) magnetic field perturbation normal to edge drives reconnection at q=4**
  - $B_{r,1}(r=a,\theta,z)=B_{ext}\, e^{i[m\theta+(n/R_0)z]}$
- **Equilibrium axial flow profile is uniform through resonant surface and decreases to zero at boundary as Gaussian**

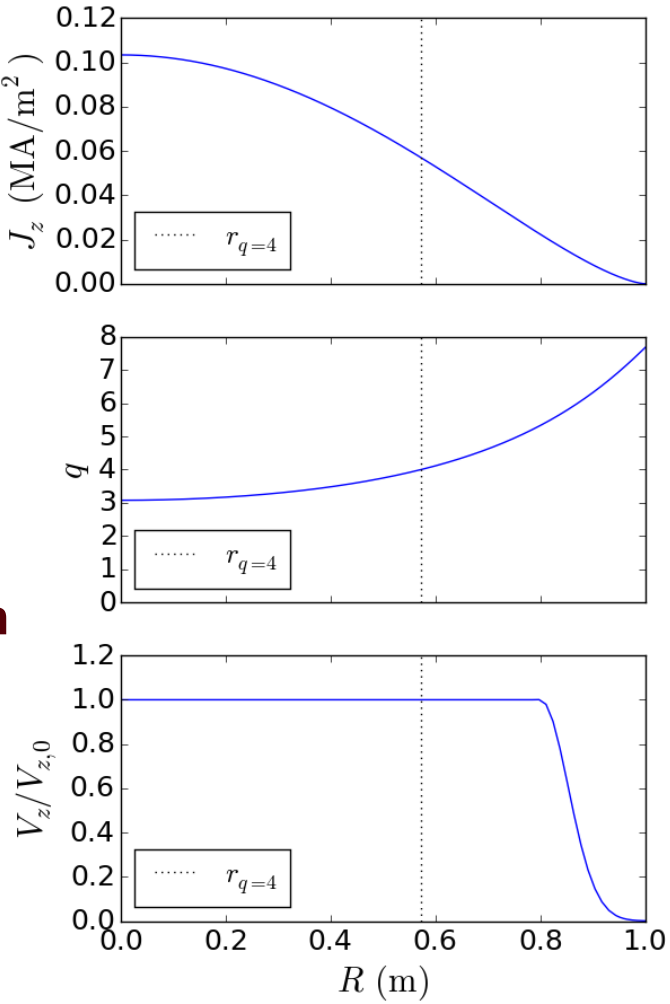

Cylindrical Benchmark Parameters Chosen to Study Visco-Resistive Physics

- **Constant β = 8x10^{-4}, constant n = 10^{19} m^{-3}, constant D$_n$ = 2 m^2/s, isotropic χ = 2 m^2/s**
- **Multiple formulations for Lundquist number**
  - S_G based on background axial field $S_G = a\frac{B_{z0}}{\eta}\sqrt{\frac{\mu_0}{\rho}} = 3.45 \times 10^6$
  - S_L based on reconnecting field $S_L = \frac{nsr_s^2}{R_0}\frac{B_{z0}}{\eta}\sqrt{\frac{\mu_0}{\rho}} = 1.27 \times 10^5$, with $s = \frac{r}{q}\frac{dq}{dr}\Big|_{r_s}$ and axial mode n
- **Magnetic Prandtl number P$_m$ = 1**
  - τ_{VR}= 2.104 τ_A $S_L^{2/3}P_m^{1/6}$ = 6.85x10^{-3} s
- **Edge resistivity and viscosity profiles ~[1+($\Delta_{vac}^{1/2}$-1)*(r/a)$^{\Delta_{exp}}$]^2**
  - Δ_{vac} =1000 increasing diffusivity, Δ_{exp} =25 for thin edge region

NIMROD and M3D-C^1 Compute Consistent Time-Asymptotic States

Vacuum Field | Penetrated Field | Screened Field (v_z =10 km/s)

NIMROD

M3D-C^1

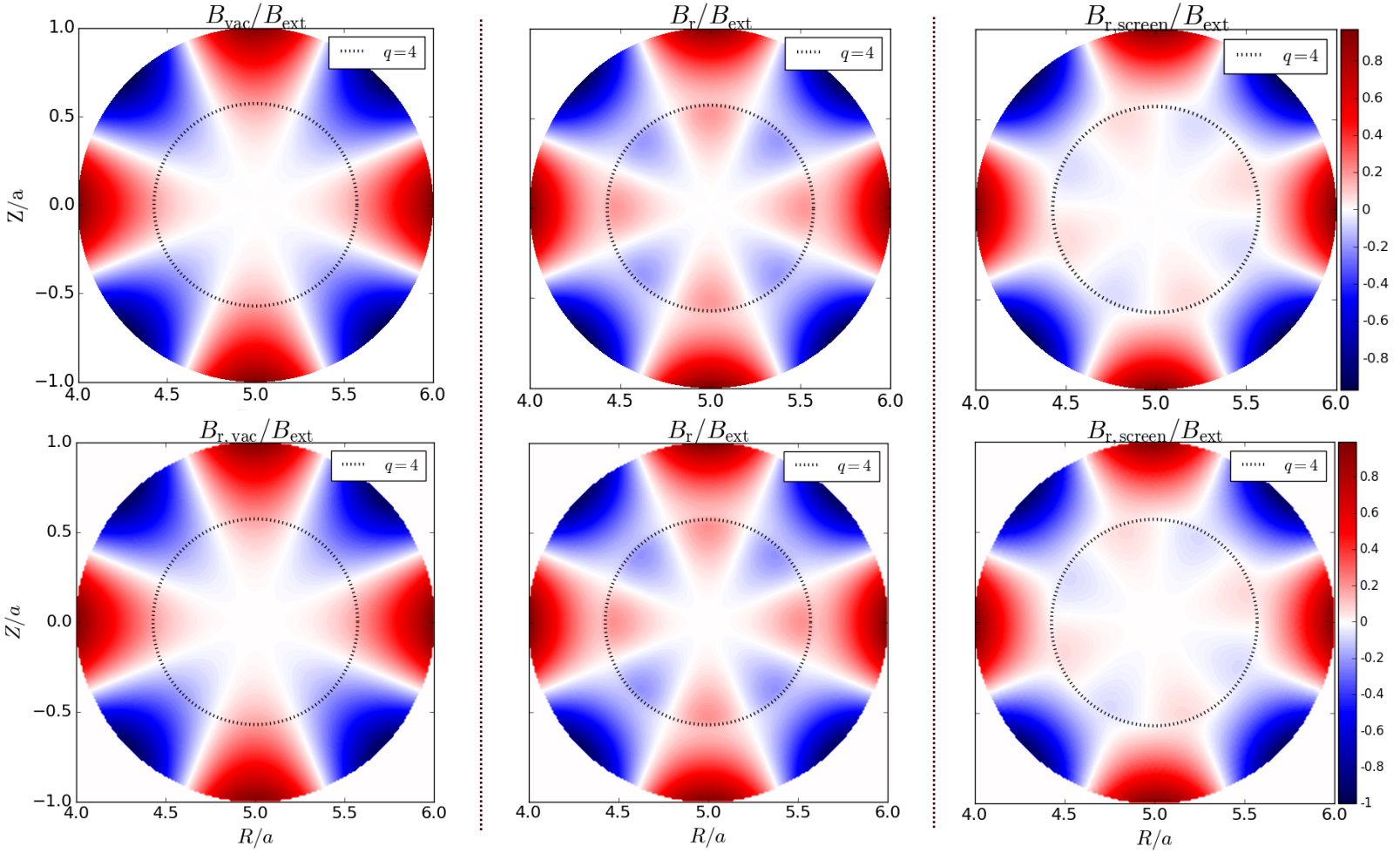

NIMROD and M3D-C[1] Linear Computations Exhibit Flow-Screened Mode Structure

- **Excellent agreement between codes for all tested v_z**
  - Phase given by

$$\arctan\left\{\frac{\Im[B_{r,1}(r_s,\theta)]}{\Re[B_{r,1}(r_s,\theta)]}\right\} - \arctan\left\{\frac{\Im[B_{r,1}(a,\theta)]}{\Re[B_{r,1}(a,\theta)]}\right\}$$

- **Alfvén resonances appear for**

$$\tau_A k_z v_{z,0} S^{1/3} \geq 1$$

NIMROD

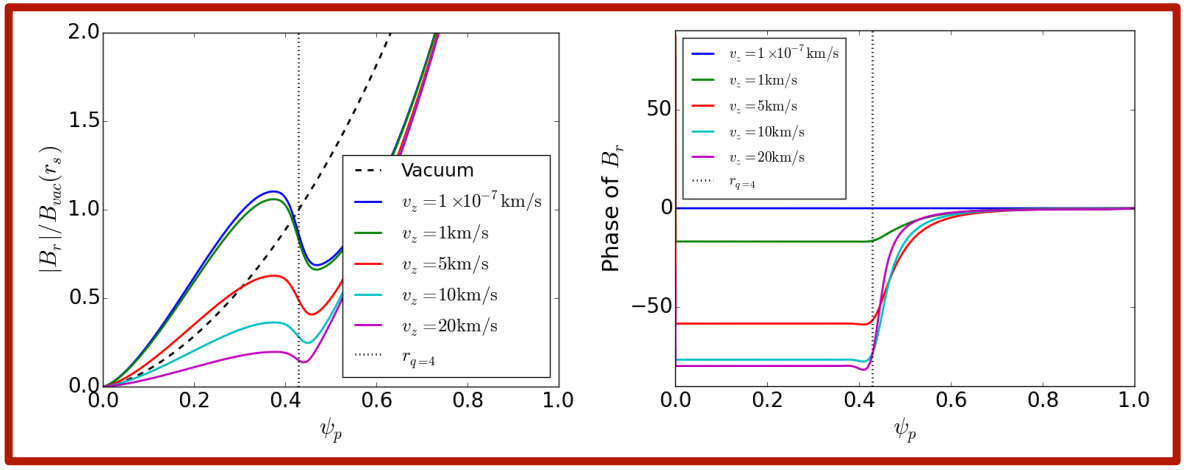

M3D-C[1]

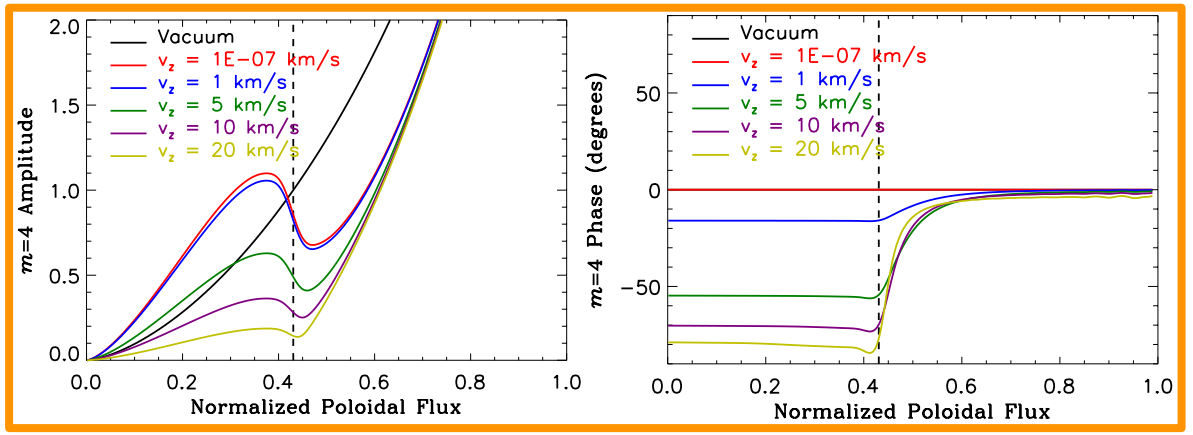

Linear Field Response Is Flow-Screened According to Time-Asymptotic Theory

- **Assume total flux function is linearly composed of forced-tearing plasma response and shielded components:**
  $\psi_{tot} = \psi_T + \psi_S$ **for** $\mathbf{B} = \hat{z}\times\nabla\psi$
  - Boundary conditions on shielded solution: $\psi_S(r\le r_s)=0$, $\psi_S(r=a)=\psi(a)$
  - Boundary conditions on tearing solution: $[\![\psi_T]\!]_{rs}=0$, $\psi_T(r=a)=0$
- **Asymptotic matching across rational surface yields [Fitzpatrick, POP (1994)]:** $i\omega\tau_\delta\psi(r_s) = \psi(r_s)r_s\Delta' + \psi(a)r_s\Delta'_{ext}$
  - $\tau_\delta = \tau_{VR}$ for VR regime
- **RESTER evaluates external forcing as** $r_s\Delta'_{ext} = 0.518$
- **Field response is given by** $$B_{res} = \frac{r_s\Delta'_{ext}}{-r_s\Delta' - i\omega_0\tau_{VR}}B_{ext}$$

Flow Screening Computations Agree Between Codes and Trend with Analytic Predictions

- **Excellent agreement between codes, which trends with linear, time-asymptotic, analytic theory**
  - $\tau_{\mathrm{VR}} = 5.44 \times 10^3 \tau_{\mathrm{A}}$
  - $\tau_{\mathrm{A}} = (R_0/n\hat{s})(\sqrt{\mu_0 \rho}/B_{z0}) = 1.29 \mu\mathrm{s}$
- **Code results agree with each other better than with analytics**
  - Computation parameters close to nexus of different dissipative regimes
  - Analytics for asymptotic VR regime

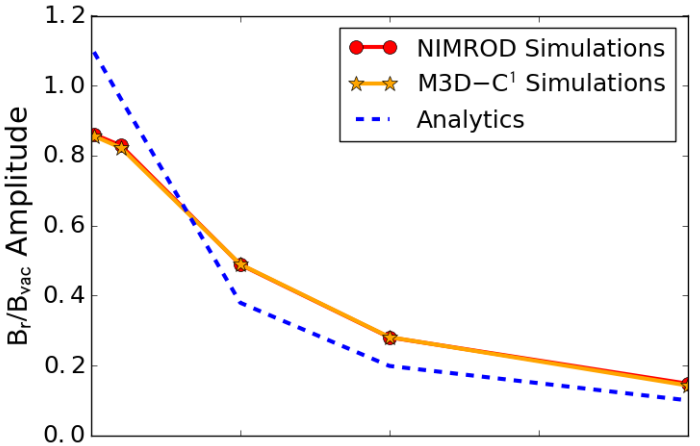

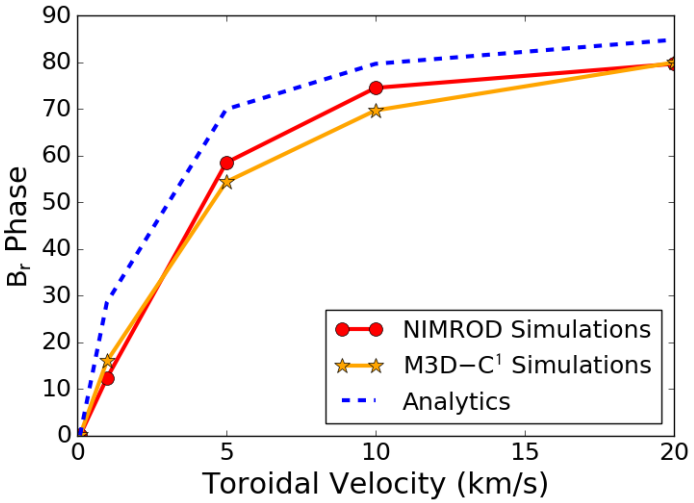

Quasilinear Poloidal and Axial Torque Balance Gives Rise to Bifurcation

- **Integrating θ, z components of J×B and $\nabla\cdot\rho\nu\nabla\mathbf{v}$ over θ, z and radially about r_s yields time-asymptotic n = 0 electromagnetic and viscous torques [Fitzpatrick, NF (1993)]**

$$\delta T_{\mathrm{EM},\theta} = \frac{-8\pi^2 R_0 r_s^2}{m} \frac{(r_s \Delta'_{\mathrm{ext}})\omega_{\mathrm{res}}\tau_{\mathrm{VR}}}{(-r_s\Delta')^2 + (\omega_{\mathrm{res}}\tau_{\mathrm{VR}})^2} \frac{B_{\mathrm{ext}}^2}{\mu_0} \qquad \delta T_{\mathrm{EM},z} = \frac{n}{m}\delta T_{\mathrm{EM},\theta}$$

$$\delta T_{\mathrm{VS},\theta} = -4\pi^2 R_0 r_s^2 \mu(r_s)\left[1 + \frac{1}{\mu(r_s)\int_{r_s}^{a}\frac{dr'}{r'\mu(r')}}\right]\Delta\Omega_\theta(r_s) \qquad \delta T_{\mathrm{VS},z} = \frac{-4\pi R_0^3}{\int_{r_s}^{a}\frac{dr'}{r'\mu(r')}}\Delta\Omega_z(r_s)$$

$$\equiv \mu_\theta \Delta\Omega_\theta(r_s) \qquad \equiv \mu_z \Delta\Omega_z(r_s)$$

  - Where $\omega_{\mathrm{res}} - \omega_0 = m\Delta\Omega_\theta(r_s) + n\Delta\Omega_z(r_s)$ is the flow response at r_s

- **Torque balance in θ, z yields cubic relation in ω_{res}**

$$\frac{\omega_0}{\omega_{\mathrm{res}}} - 1 + \omega_0\omega_{\mathrm{res}}\tau'^2_{\mathrm{VR}} - \omega_{\mathrm{res}}^2\tau'^2_{\mathrm{VR}} = \frac{-8\pi^2 R_0 r_s^2 \tau_{\mathrm{VR}}}{m^2}\left(\frac{\Delta'_{\mathrm{ext}}}{-\Delta'}\right)^2\left[\frac{m^2}{\mu_\theta} + \frac{n^2}{\mu_z}\right]\frac{B_{\mathrm{ext}}^2}{\mu_0}$$

  where $\tau'_{\mathrm{VR}} = \dfrac{\tau_{\mathrm{VR}}}{-r_s\Delta'}$

- **Bifurcation when initial angular frequency exceeds** $\omega_{0,\mathrm{crit}} = \dfrac{3\sqrt{3}}{\tau'_{\mathrm{VR}}}$

Poloidal Flow Response Dominates Axial Flow Response in Mode Penetration

- **Flow response is localized to the rational surface**
- **Poloidal flow response dominates due to smaller moment arm for poloidal viscous torque**
  - Flow response larger by $v_{\theta,1} \simeq \frac{m}{n}\frac{R_0}{r_s} v_{z,1}$
    - μ_θ = -7.82x10^{-6}, μ_z = -4.32x10^{-4}
  - *Neither cylindrical geometry nor visco-resistive MHD model contains physics of experimentally observed poloidal flow damping*
- **v_z for r<r_s is relaxing toward flat profile in time-asymptotic state**

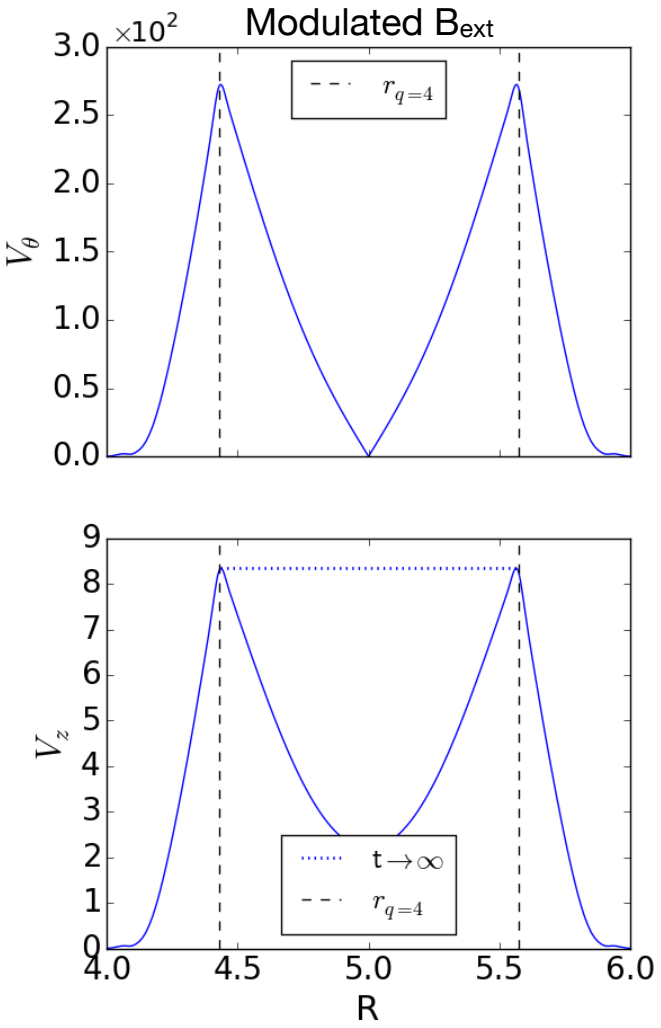

Rotating Applied Field Avoids Instability Driven by Flow Profile

- **Rotating wall B_{ext} or flowing plasma equally modulate applied field at r_s**
  - $B_{r,1} \sim B_{ext}\, e^{i\omega t}$, $\omega = \mathbf{k}\cdot\mathbf{v}_{wall}$
- **Axial flow response with equilibrium flow profile is qualitatively different from rotating B_{ext} (left figures)**
  - Magnitude of axial flow response increases with B_{ext}
    - Shown for $B_{ext} = 10^{-3}\, B_{norm}$
  - Appearance of boundary layer in rotating B_{ext} case
- **Linear (top right) and nonlinear (bottom right) flow-scaling of field response are largely unchanged for Galilean transformation**
  - Poloidal flow response is dominant in nonlinear response

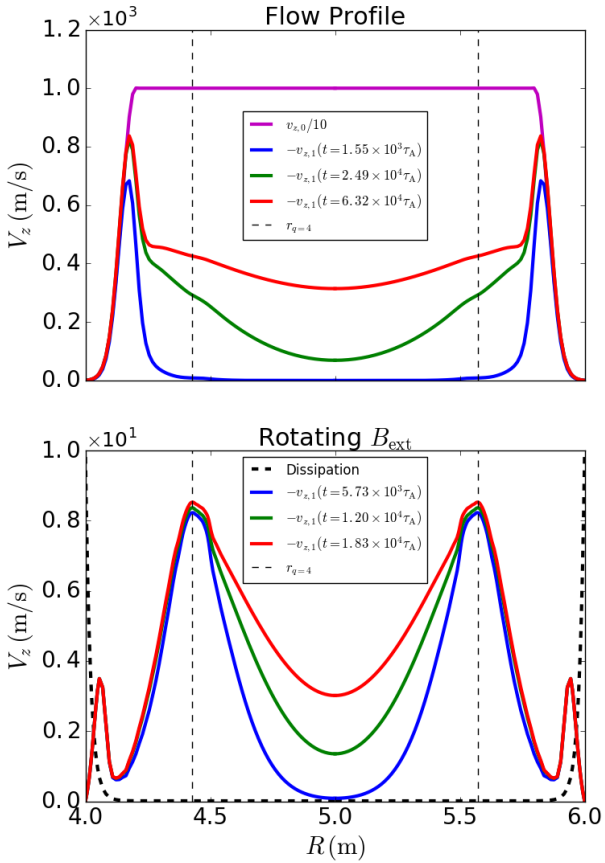

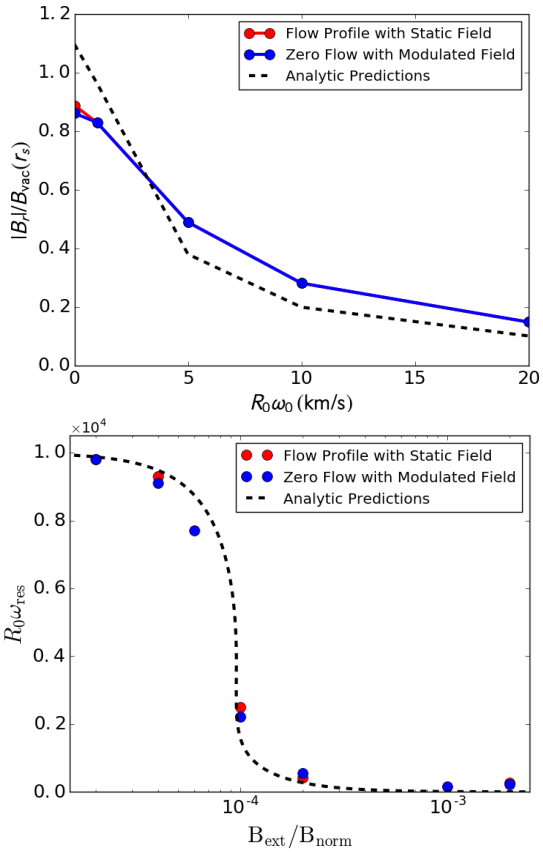

Nonlinear Mode Penetration in Cylindrical Computations is Consistent With Analytics

- **Time-asymptotic flow at r_s as a function of applied field is shown by red data**
  - Plasma stationary with modulated applied field
    - $B_{r,1}(\mathbf{r},t)=B_r(\mathbf{r})[1-e^{-t/\tau_{nw}}]e^{i\omega t}$
    - Applied field modulated at $\omega_0 = 2$ krad/s > $\omega_{0,crit} = 1.92$ krad/s

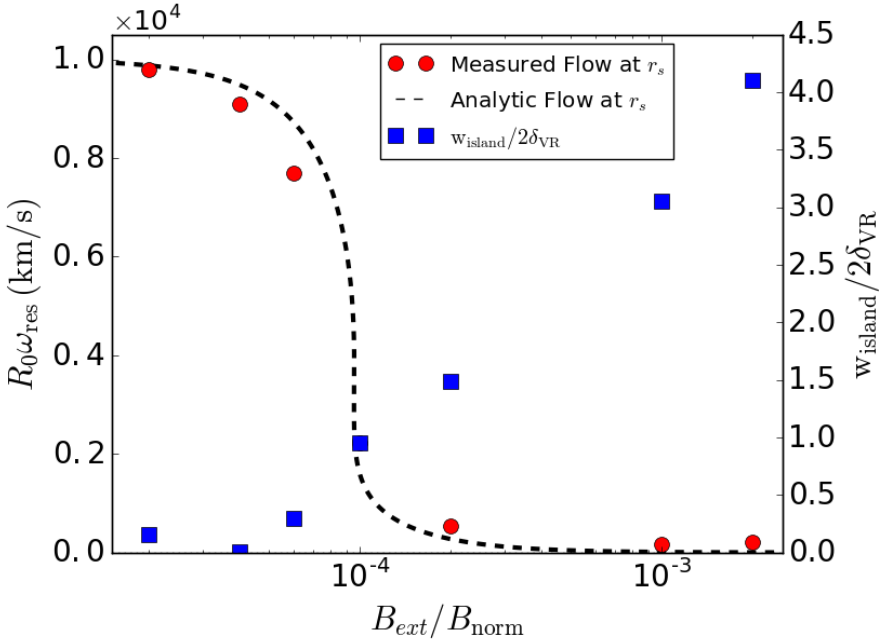

- **Measured island width (blue data) increases rapidly with applied field for penetrated modes**
- **Excellent agreement between computation and analytic predictions**
  - Quasilinear theory holds well considering island exceeds visco-resistive linear layer width δ_{VR}

Mode Penetration and Unlocking Correlate with Analytical Predictions

- **Quasilinear force balance yields**
  $B_{ext,pen\{unlock\}} = 11.6\,\{5.33\} \times 10^{-5}\, B_{norm}$
  - Response curve for $P_m = 10$ on top right
- **Bottom plots show mode penetration (left) and unlocking (right)**
  - Deviation from analytics consistent with increased field response
- **Similar to slab geometry, unlocking island rotates relative to external field**
  - Leading to increased flow screening

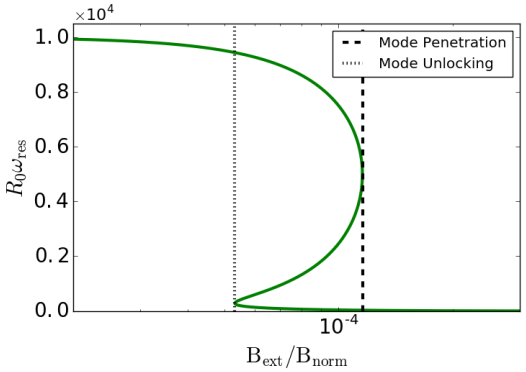

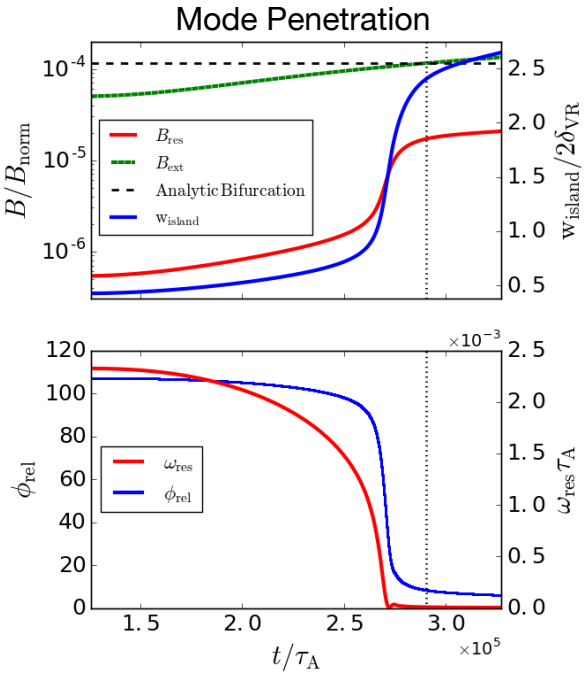

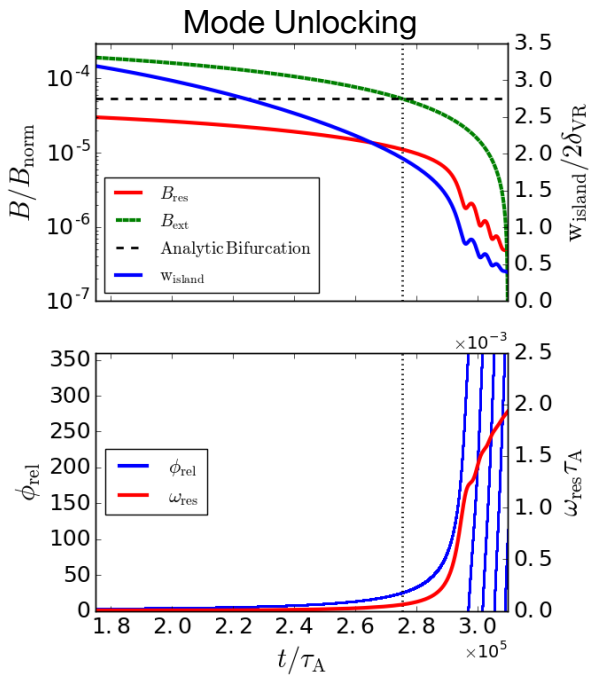

Ongoing and Future Work

- **Nonlinear cylindrical benchmarking with NIMROD and M3D-C[1]**
- **Explore various physics questions in the cylindrical geometry**
  - Nonlinear coalescence process: driving n=1 by applying n=2
  - Two-fluid effects on linear and nonlinear FMR dynamics
- **Begin to model RMPs in toroidal geometry**
  - Circular cross section test equilibrium (figure on right)
  - Well-diagnosed DIII-D experimental cases (Shafer L-mode discharges)

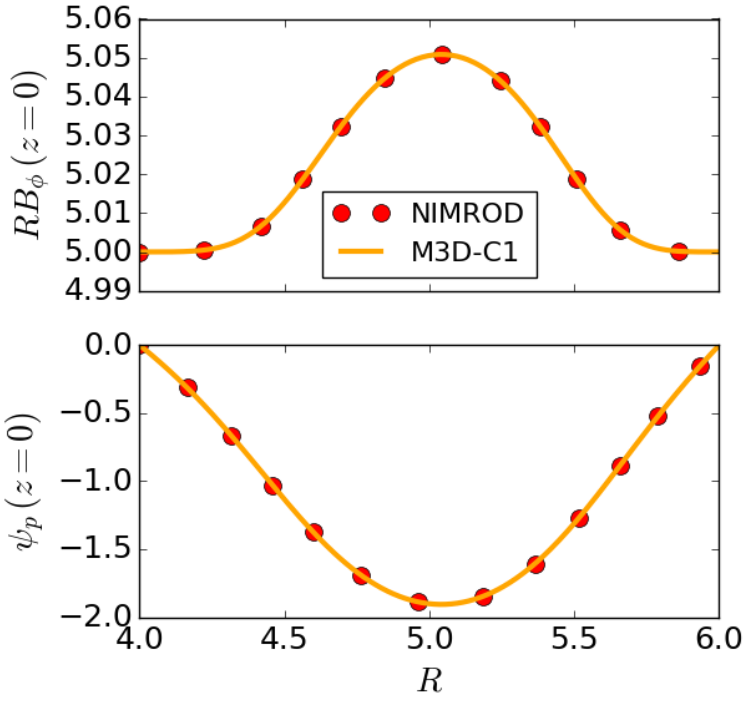

Conclusions

- **Nonlinear NIMROD computations agree with analytics of force balance which describe mode penetration bifurcation**
  - Mode penetration and unlocking exhibit hysteresis depending on profiles of initial flow and dissipation
  - Nonlinear field response increased compared to linear field response
  - *M. T. Beidler, J. D. Callen, C. C. Hegna, and C. R. Sovinec, "Nonlinear Modeling of Forced Magnetic Reconnection in Slab Geometry with NIMROD," report UW-CPTC 17-1, 7 March 2017, available via www.cptc.wisc.edu, Accepted to Physics of Plasmas*
- **Cylindrical linear benchmark with NIMROD and M3D-C^{1}exhibits excellent agreement between codes**
  - Nonlinear code benchmarks are underway

Electronic Paper Request

Beidler et al., Accepted to *Physics of Plasmas*

- Name/Email:
- _____
- _____
- _____
- _____
- _____
- _____
- _____
- _____
- _____
- _____
- _____
- _____
- _____
- _____
- _____
- _____
- _____
- _____